Quantum Chemical Study, Natural Bond Orbital Analysis and Nonlinear Optical Properties of a Series of Unsymmetrical TTFs Bearing one Fused Pyrazine Rings

Abbaz T[1]*, Bendjeddou A[1], Villemin D[2]

[1]Laboratory of Aquatic and Terrestrial Ecosystems, Org. and Bioorg. Chem. Group, University of Mohamed-Cherif Messaadia, Souk Ahras, 41000, Algeria

[2]Laboratory of Molecular and Thio-Organic Chemistry, UMR CNRS 6507, INC3M, FR 3038, Labex EMC3, ensicaen & University of Caen, Caen 14050, France

Abstract Density functional theory calculation with B3LYP using 6-31G(d,p) basis set have been used to determine ground state molecular geometries. The first order hyperpolarizability (β_0) and related properties (β, α_0 and $\Delta\alpha$) of pyrazino-fused TTFs **1-4** is calculated using B3LYP/6-31G(d,p) method on the finite-field approach. The stability of molecule has been analyzed by using NBO/NLMO analysis. Molecular electrostatic potential (MEP) surface was plotted over the geometry primarily for predicting sites and relative reactivities towards electrophilic and nucleophilic attack. The delocalization of electron density of various constituents of the molecule has been discussed with the aid of NBO analysis. The electronic properties, such as excitation energies, HOMO and LUMO energies, were calculated bysame method cited above.

Keywords tetrathiafulvalenes; density functional theory; computational chemistry; electronic structure; quantum chemical calculations

1. Introduction

Heterocyclic Chemistry is an integral part of organic chemistry and constitutes a considerable part of the syllabus for undergraduate and graduate students throughout the world. Heterocyclic chemistry deals with heterocyclic compounds which constitute about sixty-five percent of organic chemistry literature. Heterocyclic compounds are widely distributed in nature which are essential to life [1].

Heterocyclic compounds have a wide range of application: they are predominant among the type of compounds used as pharmaceuticals [2], as agrochemicals and as veterinary products. They also find applications as sensitizers, developers, antioxidants, as corrosion inhibitors, as copolymers, dyestuff [3] .They are used as vehicles in the synthesis of other organic compounds.

Nitrogen-containing compounds are privileged heterocyclic scaffold due to their biological and pharmaceutical activities [4]. They are always signified a subject of great interest due to their ubiquity in nature and massive presence as part of the skeletal backbone of many therapeutic agents.

In the recent years, density functional theory (DFT) has been extensively used in theoretical modeling. DFT offers a better compromise between computational cost and accuracy for medium size molecules, and hence it has been successfully applied in many previous studies [5-7].

In this work, we have presented a detailed study of various aspects of pyrazino-fused TTFs **1-4** described in literature [8]. Optimized structural parameters, natural bond orbital (NBO) analysis, nonlinearoptical (NLO) properties, chemical reactivity and Fukui functions are obtained using the Density Functional Theory (DFT), performing B3LYP/6-31G(d,p) level of calculations.

2. Materials and Methods

Calculations of the pyrazino-fused TTFs **1-4** were carried out using Gaussian 09 software [9] by utilizing Becke's three parameter hybrid models with the Lee-Yang-Parr correlation functional (B3LYP) method. The 6-31G(d,p) basis set was employed to predict the molecular structure shown in Fig 1. The optimized geometrical parameters (B3LYP) are given in Tables 1-4. The assignments of the calculated wave numbers are aided by the animation option of GAUSSVIEW program [10].

3. Results and Discussion

3.1. Molecular Geometry

The most relevant structural parameters (bond lengths, bond angles and dihedral angles) of title compound were determined by DFT calculations using B3LYP/ 6-31G(d, p) as basis set which are given in Tables 1-4. Geometry optimization was carried out without any symmetry constraints. The atoms numbering of molecule used in this paper is reported in Fig 1.
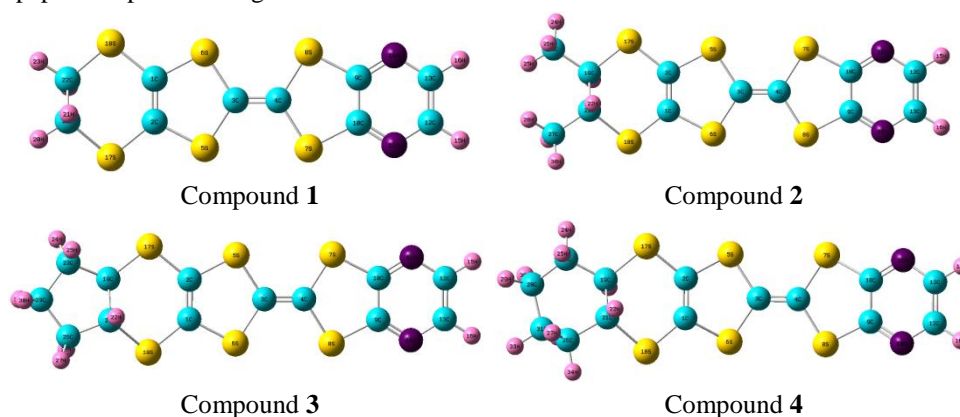

Compound **1**   Compound **2**

Compound **3**   Compound **4**

*Figure 1: Optimized molecular structure of pyrazino-fused TTFs **1-4***

Table 1: Optimized geometric parameters of compound **1**

Bond Length(Å)		Bond Angles(°)		Dihedral Angles(°)	
R(13,16)	1.086	A(7,10,9)	117.065	D(8,9,14,13)	179.968
R(12,13)	1.389	A(7,10,11)	120.952	D(16,13,14,9)	179.988
R(13,14)	1.346	A(2,17,19)	100.425	D(18,1,6,3)	179.101
R(9,14)	1.321	A(17,19,21)	109.843	D(6,1,18,22)	165.827
R(9,10)	1.415	A(12,13,16)	121.305	D(17,2,5,3)	179.099
R(8,9)	1.767	A(12,13,14)	121.954	D(2,17,19,20)	168.616
R(4,8)	1.787	A(14,13,16)	116.740	D(17,19,22,23)	171.798
R(3,4)	1.349	A(9,14,13)	116.063	D(21,19,22,24)	175.644
R(3,6)	1.781	A(3,4,7)	122.218	D(17,19,22,24)	51.549
R(1,18)	1.775	A(7,4,8)	115.562	D(4,7,10,11)	179.964
R(2,5)	1.780	A(1,6,3)	95.484	D(1,18,22,19)	49.318
R(18,22)	1.832	A(17,19,20)	103.849	D(1,18,22,23)	168.609
R(22,23)	1.094	A(17,19,22)	113.132	D(20,19,22,23)	56.142
R(19,22)	1.528	A(19,22,23)	110.046	D(5,2,17,19)	165.818
R(22,24)	1.091	A(23,22,24)	108.545	D(2,17,19,22)	49.326

Table 2: Optimized geometric parameters of compound **2**

Bond Length(Å)		Bond Angles(°)		Dihedral Angles(°)	
R(12,15)	1.086	A(11,12,15)	116.724	D(18,1,6,3)	179.322
R(12,13)	1.389	A(7,10,11)	120.958	D(6,1,18,21)	165.804
R(11,12)	1.346	A(7,10,9)	117.061	D(17,2,5,3)	179.312
R(10,11)	1.320	A(3,4,7)	122.224	D(5,3,4,8)	180.051
R(7,10)	1.767	A(4,3,5)	122.932	D(2,17,19,23)	172.401

R(9,10)	1.416	A(5,3,6)	114.134	D(17,19,21,27)	170.888
R(3,4)	1.349	A(1,2,5)	117.513	D(20,19,23,25)	55.437
R(4,8)	1.787	A(2,5,3)	95.418	D(20,19,23,26)	176.226
R(3,5)	1.781	A(17,19,20)	107.674	D(21,19,23,24)	174.316
R(1,2)	1.334	A(17,19,21)	112.093	D(21,19,23,26)	54.058
R(2,17)	1.770	A(17,19,23)	104.842	D(18,21,27,28)	170.803
R(17,19)	1.851	A(20,19,23)	109.677	D(18,21,27,30)	51.850
R(19,23)	1.535	A(19,23,25)	110.493	D(22,21,27,29)	176.230
R(23,24)	1.093	A(21,27,29)	111.363	D(23,19,21,27)	52.547
R(23,25)	1.092	A(29,27,30)	108.129	D(4,7,10,11)	179.989

Table 3: . Optimized geometric parameters of compound **3**

Bond Length(Å)		Bond Angles(°)		Dihedral Angles(°)	
R(13,16)	1.086	A(11,12,15)	116.749	D(6,1,18,21)	165.683
R(13,14)	1.346	A(11,12,13)	121.946	D(17,2,5,3)	178.997
R(14,9)	1.321	A(12,13,16)	121.303	D(5,2,17,19)	165.696
R(12,13)	1.389	A(7,10,11)	120.965	D(5,3,4,8)	179.979
R(8,9)	1.768	A(8,9,10)	117.065	D(6,3,4,7)	179.983
R(4,8)	1.787	A(3,4,7)	122.224	D(4,7,10,11)	179.945
R(3,4)	1.349	A(5,3,6)	113.979	D(20,19,21,22)	168.956
R(3,5)	1.780	A(4,3,5)	123.010	D(20,19,21,18)	48.019
R(9,10)	1.416	A(1,2,17)	129.231	D(17,19,23,24)	79.786
R(21,22)	1.094	A(2,5,3)	95.619	D(20,19,23,29)	81.370
R(21,26)	1.539	A(17,19,20)	108.280	D(19,21,26,28)	83.046
R(17,19)	1.830	A(17,19,23)	112.189	D(19,23,29,30)	134.393
R(1,2)	1.347	A(20,19,21)	109.269	D(25,23,29,31)	135.254
R(23,29)	1.557	A(25,23,29)	110.462	D(2,17,19,21)	49.152
R(1,18)	1.778	A(30,29,31)	106.864	D(23,19,21,26)	44.048

Table 4. Optimized geometric parameters of compound **4**

Bond Length(Å)		Bond Angles(°)		Dihedral Angles(°)	
R(12,15)	1.086	A(11,12,15)	116.736	D(6,1,2,17)	175.449
R(12,13)	1.396	A(11,12,13)	121.984	D(6,1,18,21)	178.575
R(10,11)	1.321	A(10,11,12)	116.007	D(17,2,5,3)	171.262
R(9,10)	1.415	A(9,10,11)	122.005	D(5,2,17,19)	153.897
R(7,10)	1.770	A(4,7,10)	94.609	D(6,3,4,7)	178.081
R(3,4)	1.349	A(7,4,8)	115.241	D(4,3,6,1)	161.129
R(3,5)	1.778	A(3,4,6)	123.330	D(3,4,7,10)	168.244
R(1,2)	1.348	A(5,3,6)	112.933	D(4,8,9,14)	173.980
R(2,17)	1.772	A(1,2,5)	117.103	D(24,23,28,31)	148.973
R(17,19)	1.840	A(2,1,18)	129.352	D(14,9,10,7)	178.244
R(19,20)	1.093	A(2,1,6)	116.713	D(10,11,12,15)	179.912
R(19,21)	1.543	A(2,17,19)	98.370	D(1,18,21,26)	165.793
R(19,23)	1.533	A(17,19,20)	106.447	D(23,19,21,22)	163.037
R(1,18)	1.774	A(20,19,23)	109.553	D(18,21,26,27)	136.119
R(28,31)	1.545	A(26,31,28)	111.380	D(19,21,26,34)	144.388

3.2. Molecular Electrostatic Potential (MEP)

Molecular electrostatic potential surface (MEPS) allows us to visualize variably charged regions of a molecule [11,12]. Knowledge of the charge distributions can be used to determine how molecules interact with one another. To make the electrostatic potential energy data easy to visualize and interpret, a colour spectrum, with red as the lowest electrostatic potential energy value and blue as the highest, is employed to convey the varying

intensities of the electrostatic potential energy values. They are often used for qualitative interpretation of electrophilic and nucleophilic reactions. Potential increases in the ordered < orange < yellow < green < blue. Such potential surfaces correlate the total charge distribution with the dipole moment, partial charges, electro-negativity and chemical site of reactivity of a molecule [13]. It can be seen from the Fig 2.
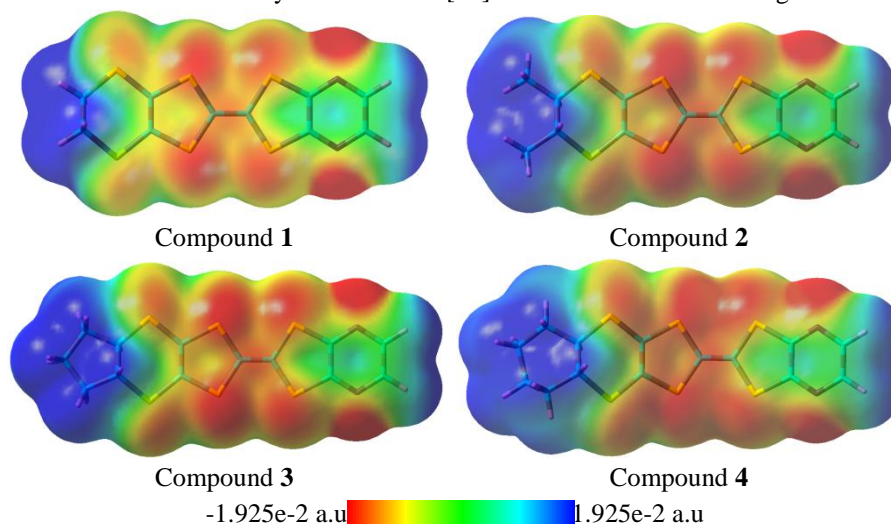

Compound **1**   Compound **2**

Compound **3**   Compound **4**

-1.925e-2 a.u ▬▬▬▬▬ 1.925e-2 a.u

*Figure 2: Molecular electrostatic potential surface of pyrazino-fused TTFs**1-4***

As seen from the figure **2** that, in all molecules, the regions exhibiting the negative electrostatic potential are localized near the TTF core and nitrogen atom that contains the alkyne function while the regions presenting the positive potential are localized vicinity of the hydrogen atoms of alkyl and cycled groups.

3.3. Frontier Molecular Orbital's (FMOs)

To explain several types of reactions and for predicting the most reactive position in conjugated systems, molecular orbital and their properties such as energy are used [14]. The highest occupied molecular orbital (HOMO) and lowest unoccupied molecular orbital (LUMO) are the most important orbital in a molecule. The eigenvalues of HOMO and LUMO and their energy gap reflect the biological activity of the molecule. A molecule having a small frontier orbital gap is more polarizable and is generally associated with a high chemical reactivity and low kinetic stability [14-19]. HOMO, which can be thought the outer orbital containing electrons, tends to give these electrons as an electron donor and hence the ionization potential is directly related to the energy of the HOMO. On the other hand LUMO can accept electrons and the LUMO energy is directly related to electron affinity [18,19]. Two important molecular orbital (MO) were examined for the compound **2** with a small energy gap, the highest occupied molecular orbital (HOMO) and the lowest unoccupied molecular orbital (LUMO) which are given in Fig3.
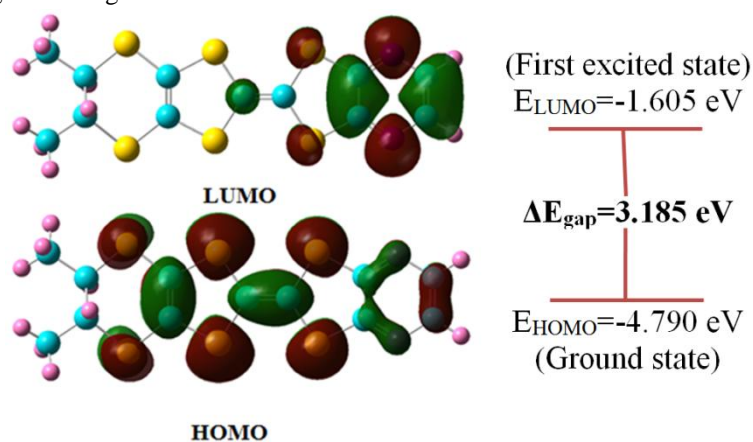

(First excited state)
$E_{LUMO}=-1.605$ eV

LUMO

$\Delta E_{gap}=3.185$ eV

$E_{HOMO}=-4.790$ eV
(Ground state)

HOMO

*Figure 3: HOMO-LUMO Structure with the energy level diagram of compound **2***

3.4. Global Reactivity Descriptors

The quantum theory of atom in molecules efficiently describes H-bonding without border. The chemical reactivity and site selectivity of the molecular systems have been determined on the basis of Koopman's theorem [20]. Energies of frontier molecular orbitals (E$_{HOMO}$, E$_{LUMO}$), have been used to calculate global reactivity descriptors such as, electronegativity (χ), chemical potential (μ), Global hardness (η), global softness (S), and electrophilicity index(ω) of pyrazino-fused TTFs**1-4** have been listed in Table 5.

Global reactivity descriptors electronegativity (χ) = -1/2(E$_{LUMO}$ + E$_{HOMO}$), chemical potential (μ) = 1/2 (E$_{LUMO}$ + E$_{HOMO}$), global hardness (η) = 1/2 (E$_{LUMO}$ −E$_{HOMO}$), global softness (S) = 1/2 η and electrophilicity index (ω) = $\mu^2/2\eta$ are highly successful in predicting global reactivity trends [21-26].

Table 5: Quantum chemical descriptors of pyrazino-fused TTFs**1-4**

Parameters	Compound 1	Compound 2	Compound 3	Compound 4
E$_{HOMO}$ (eV)	-4.859	-4.790	-4.802	-4.919
E$_{LUMO}$ (eV)	-1.641	-1.605	-1.606	-1.634
ΔE$_{gap}$ (eV)	3.218	3.185	3.196	3.285
IE (eV)	4.859	4.790	4.802	4.919
A (eV)	1.641	1.605	1.606	1.634
μ (eV)	-3.250	-3.197	-3.204	-3.276
χ (eV)	3.250	3.197	3.204	3.276
η (eV)	1.609	1.592	1.598	1.642
S (eV)	0.311	0.314	0.313	0.304
ω (eV)	3.282	3.210	3.211	4.268

As presented in table 5, the compound which have the lowest energetic gap is the compound **2** (ΔE$_{gap}$ = 3.185 eV). This lower gap allows it to be the softest molecule. The compound that have the highest energy gap is the compound **4** (ΔE$_{gap}$ = 3.285 eV).The compound that has the highest HOMO energy is the compound **2** (E$_{HOMO}$ = -4.790 eV). This higher energy allows it to be the best electron donor. The compound that has the lowest LUMO energy is the compound **1** (E$_{LUMO}$ = -1.641 eV) which signifies that it can be the best electron acceptor. The two properties like I (potential ionization) and A (affinity) are so important, the determination of these two properties allow us to calculate the absolute electronegativity (χ) and the absolute hardness (η). These two parameters are related to the one-electron orbital energies of the HOMO and LUMO respectively. Compound **2** has lowest value of the potential ionization (I = 4.790 eV), so that will be the better electron donor. Compound **1** has the largest value of the affinity (A = 1.641 eV), so it is the better electron acceptor. The chemical reactivity varies with the structural of molecules. Chemical hardness (softness) value of compound **2** (η = 1.592 eV, S = 0.314 eV) is lesser (greater) among all the molecules. Thus, compound **2** is found to be more reactive than all the compounds. Compound **4** possesses higher electronegativity value (χ = 3.276 eV) than all compounds so; it is the best electron acceptor. The value of ω for compound **4** (ω= 4.268 eV) indicates that it is the stronger electrophiles than all compounds. Compound **2** has the smaller frontier orbital gap so, it is more polarizable and is associated with a high chemical reactivity, low kinetic stability and is also termed as soft molecule.

3.5. Local Reactivity Descriptors

Fukui Function (FF) is one of the widely used local density functional descriptors to model chemical reactivity and site selectivity and is defined as the derivative of the electron density with respect to the total number of electrons N in the system, at constant external potential acting on an electron due to all the nuclei in the system. The local (condensed) Fukui functions (f_k^+, f_k^-) are calculated using the standard procedure [27–30].

$$f^+ = [q(N+1) - q(N)], \text{for nucleophilic attack,}$$

$$f^- = [q(N) - q(N-1)], \text{ for electrophilic attack,}$$

$$f^0 = [q(N+1) - q(N-1)]/2, \text{ for radical attack.}$$

Where q$_k$ is the gross electronic population of atom k in the molecule. Toro-Labbe et al. [31] have proposed a dual descriptor Δf(r), which is defined as the difference between the nucleophilic and electrophilic Fukui functions and is given by,

$$\Delta f(r) = \left[f^+(r) - f^-(r) \right]$$

If $\Delta f(r) > 0$, then the site is favored for a nucleophilic attack, whereas if $\Delta f(r) < 0$, then the site may be favored for an electrophilic attack. Fukui functions for selected atomic sites in pyrazino-fused TTFs**1-4**are shown in Tables 6-7.

Table 6: Order of the reactive sites on compounds **1** and **2**

	Compound 1					Compound 2			
Atom	4 C	1 C	2 C	3 C	**Atom**	4 C	1 C	2C	19 C
f^+	0.051	0.031	0.023	-0.023	f^+	0.052	0.037	0.026	0.000
Atom	3 C	9 C	10 C	1 C	**Atom**	3 C	9 C	10 C	2 C
f^-	0.015	0.004	0.004	0.003	f^-	0.018	0.003	0.003	0.001
Atom	1 C	4 C	2 C	3 C	**Atom**	1 C	4 C	2 C	19 C
f^0	0.017	0.014	0.013	-0.004	f^0	0.019	0.014	0.013	-0.001

Table 7: Order of the reactive sites on compounds **3** and **4**

	Compound 3					Compound 4			
Atom	4 C	2 C	1 C	21 C	**Atom**	4 C	2 C	1 C	19 C
f^+	0.050	0.022	0.013	-0.001	f^+	0.040	0.012	0.010	-0.002
Atom	3 C	9 C	10 C	2 C	**Atom**	3 C	1 C	9 C	10 C
f^-	0.017	0.004	0.004	0.001	f^-	0.021	0.010	0.003	0.003
Atom	4 C	2 C	1 C	3 C	**Atom**	4 C	1 C	2 C	3 C
f^0	0.013	0.012	0.007	0.001	f^0	0.014	0.010	0.007	0.001

From the tables 6-7, the parameters of local reactivity descriptors show that 4C is the more reactive site in compounds **1**, **2**, **3** and **4** respectively for nucleophilic attacks. The more reactive sites in radical attacks are 1C for both of compounds **1** and **2** and 4C for compounds **3** and **4** respectively. The more reactive site for electrophilic attacks is 3C for all compounds **1**, **2**, **3** and **4**respectively.

3.6. Natural Bond Orbital Analysis (NBO)
NBO analysis provides the most accurate possible 'natural Lewis structure' picture of φ, because all the orbital details are mathematically chosen to include the highest possible percentage of the electron density. A useful aspect of the NBO method is that it gives information about interactions in both filled and virtual orbital spaces that could enhance the analysis of intra- and intermolecular interactions. The second-order Fock matrix was carried out to evaluate the donor–acceptor interactions in NBO analysi s[32]. The interactions' result is the loss of occupancy from the localized NBO of the idealized Lewis structure into an empty non-Lewis orbital. For each donor (i) and acceptor (j), the stabilization energy E_2 associated with the delocalization i - j is estimated as

$$E_2 = \Delta E_{ij} = q_i \frac{F^2(i, j)}{\varepsilon_j - \varepsilon_i}$$

Where q_i is the donor orbital occupancy, ε_j and ε_i are diagonal elements and F_{ij} is the off diagonal NBO Fock matrix element. Natural bond orbital analysis provides an efficient method for studying intra- and inter-molecular bonding and interaction among bonds, and also a convenient basis for investigating charge transfer or conjugative interaction in molecular systems. Some electron donor orbital, acceptor orbital and the interacting stabilization energy resulting from the second-order micro-disturbance theory are reported [33,34]. The larger the E_2 value, the more intensive is the interaction between electron donors and electron acceptors, i.e., the more donating tendency from electron donors to electron acceptors and the greater the extent of conjugation of the whole system. NBO analysis has been performed on the molecule at the B3LYP/6-31G(d,p) level in order to elucidate the intramolecular, re-hybridization and delocalization of electron density within the molecule. Hybrids of natural bond orbitals calculated by NBO analysis are given in Tables 8-11 for the title compounds.

Table 8: Second order perturbation theory analysis of Fock matrix on NBO of compound **1**

Donor(i)	ED/e	Acceptor(j)	ED/e	E(2) Kcal/mol	E(j)-E(i) a.u	F(i.j) a.u
LP(2) S7	1.76661	π*(C10-N11)	0.42081	24.58	0.23	0.071
LP(2) S8	1.76661	π*(C9-N14)	0.42081	24.58	0.23	0.071
LP(2) S5	1.79553	π*(C3-C4)	0.41200	20.88	0.24	0.066
LP(2) S6	1.79553	π*(C3-C4)	0.41200	20.88	0.24	0.066
π(C9-N14)	1.74374	π*(C12-C13)	0.28149	20.42	0.34	0.075
π(C10-N11)	1.74374	π*(C12-C13)	0.28149	20.42	0.34	0.075
LP(2) S17	1.86798	π*(C1-C2)	0.37348	20.28	0.23	0.066
LP(2) S18	1.86798	π*(C1-C2)	0.37348	20.28	0.23	0.066
LP(2) S7	1.76661	π*(C3-C4)	0.41200	19.83	0.24	0.064
LP(2) S8	1.76661	π*(C3-C4)	0.41200	19.83	0.24	0.064
LP(2) S5	1.79553	π*(C1-C2)	0.37348	19.79	0.24	0.064
LP(2) S6	1.79553	π*(C1-C2)	0.37348	19.79	0.24	0.064
π(C12-C13)	1.64848	π*(C9-N14)	0.42081	19.36	0.26	0.064
π(C12-C13)	1.64848	π*(C10-N11)	0.42081	19.36	0.26	0.064
π(C9-N14)	1.74374	π*(C10-N11)	0.42081	15.67	0.31	0.065
π(C10-N11)	1.74374	π*(C9-N14)	0.42081	15.67	0.31	0.065
LP(1) N11	1.90852	σ*(C9-C10)	0.06158	11.29	0.85	0.088
LP(1) N14	1.90852	σ*(C9-C10)	0.06158	11.29	0.85	0.088
LP(1) N11	1.90852	σ*(C12-C13)	0.03196	8.65	0.92	0.081
LP(1) N14	1.90852	σ*(C12-C13)	0.03196	8.65	0.92	0.081

Table 9: Second order perturbation theory analysis of Fock matrix on NBO of compound **2**

Donor(i)	ED/e	Acceptor(j)	ED/e	E(2) Kcal/mol	E(j)-E(i) a.u	F(i.j) a.u
LP(2) S7	1.76665	π*(C10-N11)	0.42051	24.64	0.23	0.071
LP(2) S8	1.76665	π*(C9-N14)	0.42051	24.64	0.23	0.071
LP(2) S5	1.79619	π*(C3-C4)	0.41201	20.93	0.24	0.066
LP(2) S6	1.79619	π*(C3-C4)	0.41201	20.93	0.24	0.066
LP(2) S17	1.86835	π*(C1-C2)	0.37255	20.58	0.23	0.066
LP(2) S18	1.86836	π*(C1-C2)	0.37255	20.58	0.23	0.066
π(C9-N14)	1.74413	π*(C12-C13)	0.28146	20.41	0.34	0.075
π(C10-N11)	1.74413	π*(C12-C13)	0.28146	20.41	0.34	0.075
LP(2) S7	1.76665	π*(C3-C4)	0.41201	19.74	0.24	0.064
LP(2) S8	1.76665	π*(C3-C4)	0.41201	19.74	0.24	0.064
LP(2) S5	1.79619	π*(C1-C2)	0.37253	19.63	0.24	0.064
LP(2) S6	1.79619	π*(C1-C2)	0.37253	19.63	0.24	0.064
π(C12-C13)	1.64976	π*(C9-N14)	0.42051	19.3	0.26	0.064
π(C12-C13)	1.64976	π*(C10-N11)	0.42051	19.3	0.26	0.064
π(C9-N14)	1.74413	π*(C10-N11)	0.42051	15.64	0.31	0.065
π(C10-N11)	1.74413	π*(C9-N14)	0.42051	15.64	0.31	0.065
LP(1) N11	1.90861	σ*(C9-C10)	0.06166	11.29	0.85	0.088
LP(1) N14	1.90861	σ*(C9-C10)	0.06166	11.29	0.85	0.088
LP(1) N11	1.90861	σ*(C12-C13)	0.03193	8.64	0.92	0.081
LP(1) N14	1.90861	σ*(C12-C13)	0.03193	8.64	0.92	0.081

Table 10: Second order perturbation theory analysis of Fock matrix on NBO of compound **3**

Donor(i)	ED/e	Acceptor(j)	ED/e	E(2) Kcal/mol	E(j)-E(i) a.u	F(i.j) a.u
LP(2) S7	1.76674	π*(C10-N11)	0.42057	24.63	0.23	0.071
LP(2) S8	1.76674	π*(C9-N14)	0.42057	24.63	0.23	0.071
LP(2) S5	1.79535	π*(C3-C4)	0.41231	21.00	0.24	0.066
LP(2) S6	1.79535	π*(C3-C4)	0.412231	21.00	0.24	0.066
π(C9-N14)	0.74407	π*(C12-C13)	0.28154	20.41	0.34	0.075
π(C10-N11)	0.74407	π*(C12-C13)	0.28154	20.41	0.34	0.075
LP(2) S17	1.86766	π*(C1-C2)	0.37198	20.33	0.23	0.066
LP(2) S18	1.86766	π*(C1-C2)	0.37198	20.33	0.23	0.066
LP(2) S7	1.76674	π*(C3-C4)	0.41231	19.74	0.24	0.064
LP(2) S8	1.76674	π*(C3-C4)	0.41231	19.74	0.24	0.064
LP(2) S5	1.79535	π*(C1-C2)	0.37198	19.69	0.24	0.064
LP(2) S6	1.79535	π*(C1-C2)	0.37198	19.69	0.24	0.064
π(C12-C13)	0.64962	π*(C9-N14)	0.42057	19.30	0.26	0.064
π(C12-C13)	0.64962	π*(C10-N11)	0.42057	19.30	0.26	0.064
π(C9-N14)	0.74407	π*(C10-N11)	0.42057	15.64	0.31	0.065
π(C10-N11)	0.74407	π*(C9-N14)	0.42057	15.64	0.31	0.065
LP(1) N11	1.90859	σ*(C9-C10)	0.06165	11.29	0.85	0.088
LP(1) N14	1.90859	σ*(C9-C10)	0.06165	11.29	0.85	0.088
LP(1) N11	1.90859	σ*(12-13)	0.03195	8.64	0.92	0.081
LP(1) N14	1.90859	σ*(12-13)	0.03195	8.64	0.92	0.081

Table 11: Second order perturbation theory analysis of Fock matrix on NBO of compound **4**

Donor(i)	ED/e	Acceptor(j)	ED/e	E(2) Kcal/mol	E(j)-E(i) a.u	F(i.j) a.u
LP(2) S7	1.76407	π*(C10-N11)	0.41807	24.23	0.23	0.070
LP(2) S8	1.76391	π*(C9-N14)	0.41796	24.23	0.23	0.070
LP(2) S18	1.86200	π*(C1-C2)	0.36892	22.26	0.24	0069
π(C10-N11)	1.74252	π*(C12-C13)	0.28205	20.49	034	0.075
π(C9-N14)	1.74254	π*(C12-C13)	0.28205	20.48	0.34	0075
π(C12-C13)	1.64656	π*(C9-N14)	0.41796	19.42	0.26	0.064
π(C12-C13)	1.64656	π*(C10-N11)	0.41807	19.42	0.26	0.064
LP(2) S5	1.79893	π*(C1-C2)	0.36892	18.84	0.24	0.063
LP(2) S6	1.80033	π*(C1-C2)	0.36892	18.69	0.24	0.063
LP(2) S17	1.86723	π*(C1-C2)	0.36892	16.99	0.24	0.060
LP(2) S8	1.76391	π*(C3-C4)	0.37960	16.80	0.25	0.060
LP(2) S7	1.76407	π*(C3-C4)	0.37960	16.77	0.25	0.060
π(C9-N14)	1.74254	π*(C10-N11)	0.41807	15.74	0.31	0.065
π(C10-N11)	1.74252	π*(C9-N14)	0.41796	15.74	0..31	0.065
LP(2) S5	1.79893	π*(C3-C4)	0.37960	15.60	0.25	0.058
LP(2) S6	1.80033	π*(C3-C4)	0.37960	15.53	0.25	0.058
LP(1) N14	1.90931	σ*(C9-C10)	0.06136	11.26	0.85	0.088
LP(1) N11	1.90931	σ*(C9-C10)	0.06136	11.25	0.85	0.088
LP(1) N11	1.90931	σ*(C12-C13)	0.03205	8.67	0.91	0.081
LP(1) N14	1.90931	σ*(C12-C13)	0.03205	8.67	0.91	0.081

The intra molecular interaction for the title compounds is formed by the orbital overlap between: π(C9-N14) and π*(C12-C13) for compound **1**,π(C9-N14) and π*(C12-C13) for compound **2**, π(C9-N14) and π*(C12-C13) for compound **3** and π(C10-N11) and π*(C12-C13) for compound **4** respectively, which result into intermolecular

charge transfer (ICT) causing stabilization of the system. The intra molecular hyper conjugative interactions ofπ(C9-N14) to π*(C12-C13) for compound **1**, π(C9-N14) to π*(C12-C13) for compound **2**, π(C9-N14) to π*(C12-C13) for compound **3** and π(C10-N11) to π*(C12-C13) for compound **4** lead to highest stabilization of 20.42, 20.41, 20.41 and 20.49 kJ mol^{-1} respectively. In case of LP(2) S7 orbital to the π*(C10-N11) for compound **1**, LP(2) S7 orbital to π*(C10-N11)for compound **2**, LP(2) S7 orbital to π*(C10-N11) for compound **3,**LP(2) S7 orbital to π*(C10-N11) for compound **4** respectively, show the stabilization energy of 24.58, 24.64, 24.63 and 24.23 kJ mol^{-1} respectively.

3.7. Nonlinear Optical Properties (NLO)

The nonlinear optical activity provide useful information for frequency shifting, optical modulation, optical switching and optical logic for the developing technologies in areas such as communication, signal processing and optical interconnections [35,36]. In the presence of an applied electric field, the energy of a system is a function of the electric field. First hyperpolarizability is a third rank tensor that can be described by a $3 \times 3 \times 3$ matrix. The 27 components of the 3D matrix can be reduced to 10 components due to the Kleinman symmetry [36]. The components of β are defined as the coefficients in the Taylor series expansion of the energy in the external electric field. When the electric field is weak and homogeneous, this expansion becomes

$$E = E^{0} - \mu_i F_i - 1/2\alpha_{ij} F_i F_j - 1/6\beta_{ijk} F_i F_j F_k + ...$$

where E $_0$ is the energy of the unperturbed molecule, F $_i$ is the field at the origin, μ_i , α_{ij} , β_{ijk} and γ_{ijkl} are the components of dipole moment, polarizability, the first hyperpolarizabilities, and second hyperpolarizabilities, respectively. The total static dipole moment (μ_0), anisotropy of the polarizability (α_0), mean polarizability ($\Delta\alpha$) and the total first hyperpolarizability (β_0) using (x, y, z) components are defined as [37].

$$\mu_{tot} = \left[\mu_x^2 + \mu_y^2 + \mu_z^2\right]^{1/2}$$

$$\alpha = \left(\alpha_{xx} + \alpha_{yy} + \alpha_{zz}\right)/3$$

$$\Delta\alpha = 2^{-1/2}\left[\left(\alpha_{xx} - \alpha_{yy}\right)^2 + \left(\alpha_{yy} - \alpha_{zz}\right)^2 + \left(\alpha_{zz} - \alpha_{xx}\right)^2 + 6\alpha_{xz}^2 + 6\alpha_{xy}^2 + 6\alpha_{yz}^2\right]^{1/2}$$

$$\beta_{tot} = \left(\beta_x^2 + \beta_y^2 + \beta_z^2\right)^{1/2}$$

$$\beta_x = \beta_{xxx} + \beta_{xyz} + \beta_{xzz}$$

$$\beta_y = \beta_{yyy} + \beta_{xxy} + \beta_{yzz}$$

$$\beta_z = \beta_{zzz} + \beta_{xxz} + \beta_{yyz}$$

The total molecular dipole moment (μ), mean polarizability (α_0) and anisotropy polarizability ($\Delta\alpha$) and first hyperpolarizability (β_{total}) of diazafluorene-functionalized TTFs**1-4** are computed and are depicted in Table 12.

Table 12: The dipole moments μ (D), polarizability α, the average polarizability α (esu), the anisotropy of the polarizability Δα (esu), and the first hyperpolarizability β (esu) of pyrazino-fused TTFs**1-4**calculated by B3LYP/6-31G(d,p) method

Parameters	Compound 1	Compound 2	Compound 3	Compound 4
β_{xxx}	-60.2352	-37.4255	17.9782	3.8555
B_{yyy}	0.0001	0.0003	0.0001	-0.5881
B_{zzz}	0.0005	0.0071	0.0062	5.0111
B_{xyy}	-15.3822	-27.3564	25.8286	-29.8323
B_{xxy}	0.0007	0.0020	-0.0008	-6.1847
B_{xxz}	0.0046	0.0515	0.0473	47.3029
B_{xzz}	-3.5186	-9.0655	13.3049	-8.2854
B_{yzz}	-0.0003	-0.0017	0.0004	-0.5377
B_{yyz}	-0.0001	-0.0007	-0.0019	-2.8648
B_{xyz}	3.0813	4.2439	3.2612	2.6997

B_{tot}**(esu)x10^{-33}**	60.6725	42.2471	34.5443	16.4246
μ_x	-2.7147	-3.5083	3.5641	-3.4456
μ_y	0.0000	0.0000	0.0000	-0.0773
μ_z	0.0002	0.0012	0.0008	0.6459
μ_{tot}**(D)**	2.7147	3.5083	3.5641	3.5065
α_{xx}	-97.3777	-107.7273	-112.9914	-121.4516
α_{yy}	-154.3004	-166.7166	-172.3507	-178.6862
α_{zz}	-148.8825	-161.6619	-166.1422	-171.8623
α_{xy}	0.0000	-0.0001	-0.0001	-0.2762
α_{xz}	-0.0007	-0.0019	-0.0013	1.5112
α_{yz}	-0.4425	-0.8487	0.4906	-0.8672
α**(esu)x10^{-24}**	54.4218	56.6505	56.5114	54.2115
$\Delta\alpha$**(esu)x10^{-24}**	8.0653	8.3956	8.3750	8.0341

Since the values of the polarizabilities ($\Delta\alpha$) and the hyperpolarizabilities (β_{tot}) of the GAUSSIAN 09 output are obtained in atomic units (a.u.), the calculated values have been converted into electrostatic units (e.s.u.) (for α; 1 a.u = 0.1482 x 10^{-24} e.s.u., for β; 1 a.u = 8.6393 x 10^{-33} e.s.u.). The calculated values of dipole moment (μ) for the title compounds were found to be 2.7147, 3.5083, 3.5641 and 3.5065 D respectively, which are approximately three times than to the value for urea (μ = 1.3732 D). Urea is one of the prototypical molecules used in the study of the NLO properties of molecular systems. Therefore, it has been used frequently as a threshold value for comparative purposes. The calculated values of polarizability are 54.4218 x 10^{-24}, 56.6505 x 10^{-24}, 56.5114 x 10^{-24} and 54.2115 x 10^{-24} esu respectively; the values of anisotropy of the polarizability are 8.0653, 8.3956, 8.3750 and 8.0341 esu, respectively. The magnitude of the molecular hyperpolarizability (β) is one of important key factors in a NLO system. The DFT/6-31G(d,p) calculated first hyperpolarizability value (β) of pyrazino-fused TTFs molecules are equal to 60.6725 x 10^{-33}, 42.2471 x 10^{-33}, 34.5443 x 10^{-33} and 16.4246 x 10^{-33} esu. The first hyperpolarizability of title molecules is approximately 0.18, 0.12, 0.10 and 0.04 times than those of urea (β of urea is 343.272 x10^{-33} esu obtained by B3LYP/6-311G (d,p) method). This result indicates that pyrazino-fused TTFs**1-4**are not nonlinear.

4. Conclusion

In the present investigation density functional calculations atB3LYP/6-31G(d, p) level were carried out to study the equilibrium geometrical parameters, the charge transfer interaction, first order hyperpolarizability and the HOMO–LUMO energy gap explain the NLO activity of pyrazino-fused TTFs**1-4**.The more electronegativity is in TTF core and nitrogen atom that contains the alkyne function it the most reactive part in the molecule. The calculated first hyperpolarizability of the title compound is equal to 60.6725 x 10^{-33}, 42.2471 x 10^{-33}, 34.5443 x 10^{-33} and 16.4246 x 10^{-33} esu, which comparable with the reported values of similar derivatives and which is inferior that of the standard NLO material urea (343.272 x10^{-33}esu). We conclude that the title compound is not an attractive object for future studies of nonlinear optical properties.

References

[1]. Gupta, R.R., Kumar, M., & Gupta,V. (1998). Heterocyclic Chemistry. Springer-Verlag Berlin Heidelberg, 1-2.

[2]. Czarnik, A. (1996). Guest Editorial. Acc. Chem. Res. 29:112–113.

[3]. Kozikowski, A. (1984). Compressive Heterocyclic Chemistry. Pergamon Press, 1: 567.

[4]. Sabatini, S., Gosetto, F., Serritella, S., Manfroni, G., Tabarrini, O., Iraci, N., Brincat, J.P., Carosati, E., Villarini, M., Kaatz, G.W., & Cecchetti, V. (2012). Pyrazolo[4,3-C][1,2]Benzothiazines 5,5-Dioxide: A

Promising New Class of Staphylococcus Aureus Nora Efflux Pump Inhibitors. J. Med. Chem. 55: 3568-3572.

[5]. Srivastava, A.K., Pandey, A.K., Jain, S., & Misra, N. (2015). FT-IR Spectroscopy, Intra-Molecular C−H⋯O Interactions, HOMO, LUMO, MESP Analysis and Biological Activity of Two Natural Products, Triclisine and Rufescine. Spectrochim. Acta A, 136: 682-689.

[6]. Srivastava, A.K., & Misra, N. (2013). A Comparative Theoretical Study on the Biological Activity, Chemical Reactivity, and Coordination Ability of Dichloro-Substituted (1, 3-Thiazol-2-Yl) Acetamides. J. Chem. 92: 234-239.

[7]. Srivastava, A.K., Baboo, V., Narayana, B., Sarojini, B.K., & Misra, N. (2014). Comparative DFT Study on Reactivity, Acidity and Vibrational Spectra of Halogen Substituted Phenylacetic Acids. J. Pure Appl. Phys. 52: 507-519.

[8]. Lorcy, D., Bellec, N., Fourmigué, M., & Avarvari, N. (2009). Tetrathiafulvalene-Based Group XV Ligands: Synthesis, Coordination Chemistry and Radical Cation Salts. Coordination Chemistry Reviews, 253: 1398-1438.

[9]. Frisch, M.J., Trucks, G.W., Schlegel, H.B., Scuseria, G.E., Robb, M.A., Cheeseman, J.R., Scalmani, G., Barone, V., Mennucci, B., Petersson, G.A., Nakatsuji, H., Caricato, M., & Li, X. (2010). Gaussian 09, Revision B.01, Gaussian, Inc., Wallingford CT.

[10]. Dennington, R., Keith, T., & Millam, J. (2009). GaussView, Version 5, Semichem Inc. Shawnee Mission KS.

[11]. Weiner, K.P., Langridge, R., Blaney, M.J., Schaefer, R., & Kollman, A.P. (1982). Biophysics. Electrostatic Potential Molecular Surfaces. (Nucleic Acids/Proteins/Drug-Nucleic Acid Interactions/Protein-Ligand Interactions). Proc. Nat. Acad. Sci. U. S. A. 79: 3754-3758.

[12]. Chidangil, S., Shukla, M.K., & Mishra, P.C. (1998). A Molecular Electrostatic Potential Mapping Study of Some Fluoroquinolone Anti-Bacterial Agents. J. Mol. Model, 4: 250-258.

[13]. Kumru, M., Kucuk, V., Kocademir, M., Alfanda, H.M., Altun, A., & Sarı, L. (2015). Spec-trochim. Acta A Mol. Biomol. Spectrosc. 134: 81.

[14]. Choudhary, N., Bee, S., & Gupta, A. (2013). Comparative Vibrational Spectroscopic Studies, HOMO–LUMO and NBO Analysis of N-(Phenyl)-2,2-Dichloroacetamide, N-(2-Chloro Phenyl)-2,2-Dichloroacetamide and N-(4-Chloro Phenyl)-2,2-Dichloroacetamide Based on Density Functional Theory. Comp. Theor. Chem. 1016: 8-21.

[15]. Sinha, N., Prasad, O., Narayan, V., & Shukla, S.R. (2011). Raman, FT-IR Spectroscopic Analysis and First-Order Hyperpolarisability of 3-Benzoyl-5-Chlorouracil by First Principles. J. Mol. Simul. 37: 153-163.

[16]. Lewis, D.F.V., Loannides, C., & Parke, D.V. (1994). Interaction of a Series of Nitriles with the Alcohol-Inducible Isoform of P450: Computer Analysis of Structure-Activity Relationships. Xenobiotica, 24: 401-408.

[17]. Kosar, B.,&Albayrak,C. (2011).Spectroscopic Investigations and Quantum Chemical Computational Study of (E)-4-Methoxy-2-[(P-Tolylimino)Methyl]Phenol. Spectrochim. Acta, 78: 160-167.

[18]. Gece, G. (2008). The Use of Quantum Chemical Methods in Corrosion Inhibitor Studies. Corros. Sci. 50: 2981-2992.

[19]. Fukui, K. (1982). Role of Frontier Orbitals in Chemical Reactions. Science 218: 747-754.

[20]. Parr, R.G., & Yang, W. (1989). Density Functional Theory of Atoms and Molecules, Oxford University Press, Oxford, New York.

[21]. Pearson, R.G. (1989). Absolute Electronegativity and Hardness: Applications to Organic Chemistry. J. Org. Chem. 54: 1430-1432.

[22]. Parr, R.G., & Pearson,R.G. (1983). Absolute Hardness: Companion Parameter to Absolute Electronegativity. J. Am. Chem. Soc. 105: 7512-7516.

[23]. Geerlings, P., Proft, F.D., & Langenaeker, W. (2003). Conceptual Density Functional Theory. Chem. Rev. 103: 1793-1874.

[24]. Parr, R.G., Szentpály, L.V., & Liu, S. (1999). Electrophilicity Index. J. Am. Chem. Soc. 121: 1922-1924.

[25]. Chattaraj, P.K., Sarkar, U., & Roy, D.R. (2006). Electrophilicity Index. Chem. Rev. 106: 2065-2091.

[26]. Padmanabhan, J., Parthasarathi, R., Subramaniaan, V., & Chattaraj, P.K. (2007). Electrophilicity-Based Charge Transfer Descriptor. J. Phys.Chem. A 111: 1358-1361.

[27]. Singh, R.N., Rawat, P., & Sahu, S. (2013). Synthesis, Spectral Analysis and Study of Antimicrobial Activity of 2,5-Diformyl-1H-Pyrrole) Bis(Methan-1-Yl-1-Ylidene)Dimalonohydrazone. J. Mol. Struct. 1054–1055:123-133.

[28]. Parr, R.G., & Yang, W. (1989). Functional Theory of Atoms and Molecules, Oxford Univ. Press, N. Y.

[29]. Singh, R.N., & Rawat, P. (2013). Spectral Analysis, Structural Elucidation, and Evaluation of Both Nonlinear Optical Properties and Chemical Reactivity of A Newly Synthesized Ethyl-3,5-Dimethyl-4-[(Toluenesulfonyl)-Hydrazonomethyl]-1H-Pyrrole-2-Carboxylate Through Experimental Studies and Quantum Chemical Calculations. J. Mol. Struct. 1054–1055: 65-75.

[30]. Morell, C., Grand, A., & Toro-Labbe, A. (2005). New Dual Descriptor for Chemical Reactivity. J. Phys. Chem. A 109: 205.

[31]. Smith, B.C. (1999). Infrared Spectral Interpretation a Systematic Approach, CRC Press,Washington, DC.

[32]. Szafran, M., Komasa, A., & Adamska, E.B. (2007). Crystal and Molecular Structure of 4-Carboxypiperidinium Chloride (4-Piperidinecarboxylic Acid Hydrochloride). J. Mol. Struct. Theochem. 827: 101-107.

[33]. Schwenke, D.W., & Truhlar, D.G. (1985). Systematic Study of Basis Set Superposition Errors in the Calculated Interaction Energy of Two HF Molecules. J. Chem. Phys. 82: 2418-2427.

[34]. Andraud, C., Brotin, T., Garvia, C., Pelle, F., Goldner, P., Bigot, B., & Collet, A. (1994). Theoretical and Experimental Investigations of the Nonlinear-Optical Properties of Vanillin, Polyenovanillin, and Bisvanillin Derivatives. J. Am. Chem. Soc. 116: 2094-2101.

[35]. Geskin, V.M., Lambert, C., & Bredas, J.L. (2003). Origin of High Second- and Third-Order Nonlinear Optical Response in Ammonio/BoratoDiphenylpolyene Zwitterions: The Remarkable Role of Polarized Aromatic Groups. J. Am. Chem. Soc. 125 () 15651-15658.

[36]. Kleinman, D.A. (1962). Nonlinear Dielectric Polarization in Optical Media. Phys. Rev. 126: 1977-1979.

[37]. Karna, S. P., Prasad, P. N., & Dupuis, M. (1991). Nonlinear Optical Properties of P-Nitroaniline: An Ab Initio Time-Dependent Coupled Perturbed Hartree-Fock Study. J. Chem. Phys. 94: 1171-1181.